HHS Public Access

Author manuscript

Matrix Biol. Author manuscript; available in PMC 2019 May 29.

Published in final edited form as:

Matrix Biol. 2019 April ; 77: 41–57. doi:10.1016/j.matbio.2018.08.004.

Prostate cancer sheds the αvβ3 integrin in vivo through exosomes

Shiv Ram Krishn[a,b,†], **Amrita Singh**[a,b,†], **Nicholas Bowler**[a,b], **Alexander N. Duffy**[a,b], **Andrea Friedman**[a,b], **Carmine Fedele**[a,b], **Senem Kurtoglu**[a,b], **Sushil K. Tripathi**[c], **Kerith Wang**[d], **Adam Hawkins**[d], **Aejaz Sayeed**[a,b], **Chirayu P. Goswami**[e], **Madhukar L. Thakur**[c], **Renato V. Iozzo**[e], **Stephen C. Peiper**[e], **William K. Kelly**[d], and **Lucia R. Languino**[a,b]

[a]**Prostate Cancer Discovery and Development Program,** Thomas Jefferson University, Philadelphia, PA 19107, USA

[b]**Departments of Cancer Biology,** Thomas Jefferson University, Philadelphia, PA 19107, USA

[c]**Radiology,** Thomas Jefferson University, Philadelphia, PA 19107, USA

[d]**Medical Oncology,** Thomas Jefferson University, Philadelphia, PA 19107, USA

[e]**Pathology,** Anatomy and Cell Biology, Thomas Jefferson University, Philadelphia, PA 19107, USA

Abstract

The αvβ3 integrin has been shown to promote aggressive phenotypes in many types of cancers, including prostate cancer. We show that GFP-labeled αvβ3 derived from cancer cells circulates in the blood and is detected in distant lesions in NOD scid gamma (NSG) mice. We, therefore, hypothesized that αvβ3 travels through exosomes and tested its levels in pools of vesicles, which we designate extracellular vesicles highly enriched in exosomes (ExVs), and in exosomes isolated from the plasma of prostate cancer patients. Here, we show that the αvβ3 integrin is found in patient blood exosomes purified by sucrose or iodixanol density gradients. In addition, we provide evidence that the αvβ3 integrin is transferred through ExVs isolated from prostate cancer patient

Correspondence to Lucia R. Languino: 233 S. 10th Street, BLSB 506, Philadelphia, PA 19107, USA. Lucia.Languino@jefferson.edu.

†Equal contribution.

Authors' contributions

S.R. Krishn, A. Singh, C. Fedele, S. Kurtoglu, L.R. Languino conceptualized and designed the study.

S.R. Krishn, A. Singh, C. Fedele, S. Kurtoglu, R.V. Iozzo, L.R. Languino developed methodology.

K. Wang acquired blood specimens.

S.R. Krishn, A. Singh, N. Bowler, S. Kurtoglu, A. Friedman, C. Goswami, R.V. Iozzo, performed analysis.

S.R. Krishn, A. Singh, N. Bowler, A. Duffy, C. Fedele, A. Friedman, S. Kurtoglu, A. Sayeed, S.K. Tripathi, M.L. Thakur, R.V. Iozzo, and A. Hawkins acquired data.

S.R. Krishn, A. Singh, N. Bowler, S. Kurtoglu, A. Friedman, C. Goswami, R.V. Iozzo, and L.R. Languino interpreted the data (e.g., statistical analysis, biostatistics, computational analysis).

S.R. Krishn, A. Singh, L.R. Languino wrote the manuscript.

S.R. Krishn, A. Singh, N. Bowler, A. Duffy, A. Friedman, C. Fedele, S. Kurtoglu, A. Hawkins, K Wang, S.K. Tripathi, C. Goswami, A. Sayeed, M.L. Thakur, S.C. Peiper, W.K. Kelly, R.V. Iozzo, and L.R. Languino reviewed, and/or revised the manuscript.

S.R. Krishn, A. Singh, C. Goswami, S.C. Peiper, W.K. Kelly and L.R. Languino provided administrative, technical, or material support (i.e., reporting or organizing data, constructing databases).

Declaration of interests

The authors have declared that no conflict of interest exists.

Supplementary data to this article can be found online at https://doi.org/10.10167j.matbio.2018.08.004.

plasma to β3-negative recipient cells. We also demonstrate the intracellular localization of β3-GFP transferred via cancer cell-derived ExVs. We show that the ExVs present in plasma from prostate cancer patients contain higher levels of αvβ3 and CD9 as compared to plasma ExVs from age-matched subjects who are not affected by cancer. Furthermore, using PSMA antibody-bead mediated immunocapture, we show that the αvβ3 integrin is expressed in a subset of exosomes characterized by PSMA, CD9, CD63, and an epithelial-specific marker, Trop-2. Finally, we present evidence that the levels of αvβ3, CD63, and CD9 remain unaltered in ExVs isolated from the blood of prostate cancer patients treated with enzalutamide. Our results suggest that detecting exosomal αvβ3 integrin in prostate cancer patients could be a clinically useful and non-invasive biomarker to follow prostate cancer progression. Moreover, the ability of αvβ3 integrin to be transferred from ExVs to recipient cells provides a strong rationale for further investigating the role of αvβ3 integrin in the pathogenesis of prostate cancer and as a potential therapeutic target.

Keywords

αvβ3 integrin; Prostate cancer; Extracellular vesicles; Plasma exosomes; Abiraterone acetate; Enzalutamide

Introduction

Prostate cancer is one of the most frequently diagnosed cancers among U.S. males, accounting for 1 in 10 new cancer cases [1]. Although prostate cancer mortality has declined, treating this disease remains a challenge due to heterogeneity within prostate tumors as well as the aggressive nature of the disease [2]. Patients with metastatic prostate cancer who experience a clinical relapse after primary androgen ablation therapy are considered to have castrate resistant prostate cancer (CRPC) [3,4]. Treatment options for patients with metastatic CRPC include the androgen receptor inhibitor enzalutamide [5] and/or the androgen biosynthesis inhibitor abiraterone acetate [6].

To estimate the grade and histopathology of the tumor, patients undergo invasive procedures such as biopsy of the prostate at diagnosis; at later disease stages however, further sampling of prostate cancer is a challenge. Therefore, there is a clear unmet need for non-invasive diagnostic methods that will give us insights into more effective therapies for this disease. A common non-invasive marker such as prostate-specific antigen (PSA) is detected in the blood of prostate cancer patients; however, PSA level screening has limitations since it may be non-selective for cancer [7]. Hence, it is important to discover markers in biological fluids that may reduce or eliminate the use of invasive techniques and are highly specific in the detection of prostate cancer.

Recently, the importance of extracellular vesicles (EVs) for cancer diagnosis has drawn attention [8–13]. EVs are either released by budding of the plasma membrane (microvesicles) or are generated by the intraluminal budding of the multivesicular bodies (exosomes). EVs, particularly exosomes, also appear to hold potential as therapeutic targets in cancer since they have been shown to play a role in cell-cell communication by transferring biological material that may promote cancer progression and metastasis [14–21]. In cancer, deregulation of EVs has been shown for Glypican-1 containing vesicles that

are higher in plasma of pancreatic cancer patients compared to healthy individuals [10]. Only a few studies, conducted to identify the diagnostic potential of exosomes in cancer, have included gradient purified exosomes [10,22].

Circulating exosomes may serve as biomarkers for prostate cancer [23,24]. Studies demonstrating differential expression of miR-1290 and miR-375 [25], lncRNAs [26], survivin [8], EGFR [27], and PSA [28] in prostate cancer patient plasma exosomes have underscored the potential of plasma exosomes to be used as diagnostic and prognostic tools for prostate cancer. Additionally, large Oncosomes which are atypically large (1–10 μm diameter) prostate cancer cell-derived EVs are also being investigated as a source of prostate cancer-specific markers [29,30]. Since normal cells also release exosomes, isolation of prostate cancer-specific exosomes is required to achieve optimal biomarker specificity. In this regard, prostate specific membrane antigen (PSMA), a surface marker highly expressed in prostate cancer [31] has been shown to be useful for isolation of specific exosomes from the plasma of prostate cancer patients [32].

Among other bioactive molecules, exosomes contain integrins, which are transmembrane glycoproteins that function in concert among a multitude of molecules [33] for proper basement membrane assembly [34–38], or specific subunits partake in a number of diverse key roles [39–43], and deregulated in cancer [44–46]. Recently, it has been shown that tumor-derived exosomes containing integrins play a role in the formation of pre-metastatic niches and organotropic metastasis [16].

Many studies have shown that during prostate cancer progression, expression of integrins is altered. Examples include reduced levels of α5β1 and α7β1 integrins [47] and increased expression of αvβ1, αvβ6, and α6β1 integrins in prostate cancer, compared to healthy, tissues [45,48–50]. The αvβ3 integrin is highly up-regulated in primary epithelial cells isolated from prostate adenocarcinoma [51]; it leads to metastatic lesions, predominantly bone [52,53] and is found in exosomes [20]. Structurally, conformational changes of the αvβ3 integrin are driven primarily by force generation [54] and may act as a sensor of tissue biomechanics [55,56].

While aberrant levels of integrins have been observed in exosomes isolated from urine of patients with metastatic prostate cancer [57], from the plasma of patients with other cancers [16], or in monocytes from prostate cancer patients [58], there are no data on αvβ3 integrin expression in patients' plasma exosomes.

We hypothesized that αvβ3 propagates an aberrant phenotype through exosomes in human prostate cancer. Here, we show that prostate cancer cell-derived EVs highly enriched in exosomes (ExVs) carry αvβ3 integrin in the systemic circulation of NOD scid gamma (NSG) mice. For the first time, we show that αvβ3 integrin is expressed in sucrose or iodixanol gradient purified exosome fractions isolated from the blood of prostate cancer patients. We show that αvβ3 integrin is detected in ExVs isolated from plasma of prostate cancer patients at higher levels than in ExVs isolated from individuals not affected by cancer, and is taken up by αvβ3-negative cells in vitro. We also show increased levels of CD9 and αv and reduced levels of CD81 in ExVs from the plasma of prostate cancer

patients. Ours is the first study isolating PSMA-positive exosomes from prostate cancer patient blood. We provide evidence that αvβ3 integrin is co-expressed with PSMA, CD9, CD63, and Trop-2 in exosomes shed by prostate cancer cells in patient blood. Finally, we determine that, when second-line androgen deprivation therapy is administered to prostate cancer patients, the levels of β3, CD9, and CD63 do not appear to change.

Overall, our studies indicate that exosomal αvβ3 integrin may be a diagnostic tool for prostate cancer, and may promote cancer progression, thus rendering it a likely therapeutic target.

Results

Cancer cell-derived GFP-tagged αvβ3 integrin is expressed in ExVs in vitro and systemically circulates via ExVs in vivo

We first sought to investigate whether cancer cell-derived αvβ3 integrin is detected in vivo in distant metastasis. For this purpose, we generated prostate cancer cell lines stably expressing GFP-only (C4–2B Mock) or GFP-tagged β3 integrin (C4–2B-β3-GFP). Expression of GFP was verified by immunoblotting analysis (IB) using an antibody to GFP (Fig. 1A). A unique ~125 kDa band representing the β3-GFP is present in total cell lysates (TCL) from C4–2B-β3-GFP but not in C4–2B Mock cells where a ~27 kDa band is detected (Fig. 1A). Next, we tested in vitro whether the C4-B cancer cells, described above, shed ExVs containing GFP-αvβ3. The data show the expression of αv, β3, GFP and exosomal markers such as CD63, CD81, TSG101, and CD9 in the ExVs isolated from these cells (Fig. 1B).

We hypothesized that ExVs might carry αvβ3 in the circulation. To test this, we injected subcutaneously, C4–2B cells transfected with β3-GFP (right flank) and non-transfected DU145 cells (left flank) into ten NOD scid gamma (NSG) mice; after five weeks, we analyzed the GFP levels in murine organs using in vivo fluorescence imaging. We observe that in mice that were injected with C4–2B-β3-GFP cells, green fluorescence is localized in the prostates (n = 8/10), non-transfected DU145 tumors (n = 7/10), livers (n = 2/10) and lymph nodes (n = 2/10). Representative images of two livers, two DU145 tumors, and two prostates are shown (Fig. 1C).

We next tested the hypothesis that GFP-tagged αvβ3 integrin enriched ExVs are released from the GFP-positive tumor into the blood circulation in mice. For this, we isolated ExVs from the plasma of mice injected with C4–2B-β3-GFP cells and investigated the presence of green fluorescence signal through nanoparticle-tracking analysis (NTA) using 532 nm filter. We show the presence of GFP-positive ExVs in the circulation. The size of GFP enriched ExVs ranged between mean 72.9 to 117.1 nm, and their concentration ranged between 1.52×10^5– 3.39×10^7 particles/mL (Fig. 1D).

The αvβ3 integrin is expressed in exosomes isolated from prostate cancer patient blood

Since we have previously observed that cancer cell-derived αvβ3 integrin is packaged in exosomes [20] and appears to be circulating systemically via ExVs in mice (Fig. 1C), we investigated whether αvβ3 integrin is expressed in exosomes isolated from the blood of

prostate cancer patients. Blood samples were collected from patients with prostate cancer and processed to prepare plasma or serum. ExVs were then isolated via differential ultracentrifugation. The morphology and size distribution of ExVs were analyzed by transmission electron microscopy (TEM). TEM of prostate cancer patient ExVs revealed a round morphology and size within 100 nm (Fig. 2A). Furthermore, the ExVs were also characterized by IB revealing expression of an exosomal marker CD9 (Fig. 2B). Our results show that αvβ3 is detected in ExVs isolated from plasma of patients affected by prostate cancer (Fig. 2B).

Using a sucrose gradient analysis, we demonstrate that the exosomes isolated from the serum of prostate cancer patients float within the accepted density range of 1.13–1.19 g/mL [59,60]. αvβ3 levels are enriched in fractions five and six that have a density range of 1.15–1.17 g/mL (Fig. 2C), providing further evidence that the αvβ3 integrin is present in exosomes. We also show that the exosomal markers CD9 and FLOT1, a marker of lipid rafts also found in exosomes, are enriched in the same fractions as β3 while GM130, a Golgi marker not expressed in exosomes, is absent in those fractions (Fig. 2C).

We also report, for the first time, iodixanol gradient purification of exosomes from ExVs isolated from the plasma of prostate cancer patients. IB analysis of ten fractions from iodixanol gradient centrifugation revealed that exosomal markers CD9 and TSG101 are enriched along with αvβ3 integrin in fraction 8 (density = 1.151 g/mL) and fraction 9 (density = 1.165 g/mL) (Fig. 2D). Calnexin, an endoplasmic reticulum marker not expressed in exosomes is absent in these fractions (Fig. 2D). Regarding size distribution, the majority of exosomes in fraction 8 (mode = 102 nm) and fraction 9 (mode = 129 nm, data not shown) were within exosome size range of 50–150 nm [61] (Fig. 2E). These findings show that exosomes isolated from prostate cancer patient blood carry the αvβ3 integrin.

The αvβ3 integrin is transferred from αvβ3-positive ExVs isolated from prostate cancer patient plasma to αvβ3-negative prostate cancer cells

We have previously demonstrated that exosomes that express the αvβ3 integrin transfer this integrin to recipient tumorigenic or non-tumorigenic cells, does leading to a migratory phenotype [20].

A time course experiment ranging from 30 min to 24 h was performed to explore the minimum time required for this transfer and to estimate transferred levels of β3 upon incubation of ExVs isolated from a prostate cancer cell line, PC3, with αvβ3 negative BPH-1 cells. We determined that a low level of β3 is transferred in just 30 min and a more robust amount is transferred in 2–24 h (Fig. 3A). In contrast, cells that were incubated with PBS do not show detectable levels of β3. Similar results were obtained when C4–2B cells were used as recipient cells (data not shown).

Next, we for the first-time show ExV mediated β3-GFP internalization in a β3-negative DU145 cell line. For this, DU145 cells were incubated for 24 h with ExVs isolated from C4–2B-β3-GFP cells, and transfer of β3-GFP in DU145 cells was analyzed by confocal microscopy. An intracellular GFP signal as confirmed by *Z*-stack image analysis suggests ExV mediated transfer of β3-GFP in recipient DU145 cells (Fig. 3B, right).

Based on this observation, we sought to determine whether ExVs from the plasma of patients transfer β3 to cancer cells. We incubated C4–2B cells with ExVs isolated from patient plasma for 24 h and performed IB analysis to detect β3 levels in the recipient cells. We found that ExVs from three patients transferred αvβ3 to C4–2B cells (Fig. 3C). By comparison, C4–2B cells that are incubated with vehicle do not show detectable levels of β3. These findings suggest that during prostate cancer progression, ExVs may mediate intercellular communication by transferring αvβ3 integrin.

Since β3 is transferred from ExVs to recipient cells, we sought to investigate whether blocking the αvβ3 integrin in ExVs would affect internalization and β3 uptake in recipient cells. To block the αvβ3 integrin, we used a RGD peptide, which has been previously shown to bind to αvβ3 and block its function [51]. BPH-1 cells, which are nottumorigenic [62], were used as recipient cells; these cells were incubated for 24 h with PC3 ExVs that were pretreated with a RGD containing peptide or control RGE peptide for 1 h at 4 °C (Fig. 3D). At 24 h, IB analysis shows that the β3 levels are not affected in recipient cells incubated with GRGDSP containing peptide or control GRGESP peptide (Fig. 3D). This finding indicates that αvβ3 expressed in the ExVs does not act as a receptor for ExV internalization into the recipient cells.

CD9 and αvβ3 integrin are increased in patient plasma ExVs and are co-expressed in PSMA-positive ExVs

Next, we investigated whether there are changes in the size and cargo of vesicles isolated from plasma of patients compared to control groups. Our data show that there are no major size differences in ExVs from the prostate cancer and control groups. ExVs from the plasma of subjects not affected by cancer have a mean size of 107 nm and the prostate cancer patient plasma ExVs exhibit a mean size of 126 nm (Fig. 4A).

Since previous studies have shown that the αvβ3 integrin levels are very low in normal human prostate but are highly upregulated in primary cultures of epithelial cells from human prostate adenocarcinoma [51], we investigated whether the expression levels of β3 differed between ExVs from plasma of patients who have prostate cancer and plasma of subjects not affected by cancer. IB analysis of ExVs isolated from these plasma via ultracentrifugation show that αvβ3 levels are higher in ExVs from prostate cancer patients as compared to age-matched individuals not affected by cancer (Fig. 4B). This increase correlates with higher CD9 levels in all prostate cancer patients but inversely correlates with the levels of CD81, which are increased in all individuals not affected by cancer (Fig. 4B). av levels are increased in the majority of prostate cancer patient ExVs compared to subjects not affected by cancer. These results indicate that a sub-population(s) of ExVs enriched in β3, CD9 and αv is present in prostate cancer patient plasma as compared to age-matched control subjects.

To demonstrate that the β3 detected in exosomes from patient samples originates from prostate cancer-specific epithelial cells, we performed immunoisolation of exosomes using PSMA-conjugated magnetic beads to purify PSMA-positive exosomes and conducted IB analysis. Data from IB analysis show that PSMA positive prostate cancer patient exosomes contain β3, epithelial Trophoblastic cell-surface antigen-2 (Trop-2), exosomal markers CD9 and CD63 while expression of EpCAM is not detected (Fig. 4C). In another set of

experiments, plasma of prostate cancer patients was incubated with EpCAM-coated magnetic beads to isolate EpCAM-positive ExVs, and IB analysis was performed to detect levels of β3, PSMA, and CD9. Our data show that EpCAM-positive ExVs express β3 and CD9, while PSMA is not detected (Data not shown). Thus, our data suggest the presence of β3 integrin in two different subpopulations of ExVs (PSMA-positive and EpCAM-positive) in prostate cancer patient blood.

Based on the aberrant CD9 and CD81 protein levels in ExVs from the plasma of prostate cancer patients compared to subjects not affected by cancer (Fig. 4B), we also investigated, using the Oncomine database, whether this differential gene expression for both CD9 and CD81 also occurs in human tissues from the two groups. For CD9 (Fig. 5A–D), 14 out of 17 available datasets show no statistically significant differential gene expression between normal and cancerous tissue, while for CD81 (Fig. 5E–H), 16 out of 17 datasets show no statistically significant differential gene expression of this gene. Supplementary Table S1 shows detailed information about the datasets analyzed. Overall, the analysis of public datasets shows that the expression of CD9 or CD81 RNA levels are not different in normal and cancerous tissues, whereas our IB analysis shows that CD9 or CD81 protein levels are aberrant.

β3 levels in ExVs from castrate-resistant prostate cancer patients treated with androgen deprivation therapy

Having shown that the αvβ3 integrin levels are higher in ExVs from patients compared to subjects not affected by cancer, and knowing that increased αvβ3 integrin expression has been detected in many other tumor types, we investigated whether drug treatments with enzalutamide or abiraterone acetate, which are the standard of care for men with advanced prostate cancer, have any effect on αvβ3 integrin levels in exosomes.

The demographics and health information of prostate cancer patients are listed in Supplementary Table S2. Before analyzing the levels of β3, NTA was performed on ExVs isolated from patient sera from the following groups: subjects being either non-castrate (only leuprolide treated, designated non-treated with A or E), metastatic castrate-resistant (leuprolide+abiraterone treated, designated A); and (leuprolide+enzalutamide treated, designated E). The data show that ExVs from the three groups ranges between 92 nm to 135 nm in mean size and the concentration range between 1.71×10^8 –1.04×10^9 particles/mL (Fig. 6A). To show that abiraterone acetate or enzalutamide was effective, PSA levels were measured for patients before and after treatment. PSA levels indicate that the majority of patients respond to treatment with abiraterone acetate or enzalutamide alone (Fig. 6B).

We analyzed αvβ3 integrin and exosomal markers CD63, and CD9 expression between ExVs isolated (CD63, CD9) expression within the patient cohorts. from the plasma of non-castrate prostate cancer We find that there is no change in αvβ3 integrin, patients not treated with enzalutamide or ExVs from metastatic CRPC patients treated with the androgen receptor antagonist enzalutamide (Fig. 7) or abiraterone acetate (data not shown). Overall, these findings indicate that β3, CD63 and CD9 levels are unlikely to be informative as markers to monitor response to therapy.

Discussion

We show here, for the first time, that cancer cell-derived exosomes carry αvβ3 systemically in mice and prostate cancer patients' blood, and that αvβ3 is transferred via ExVs isolated from prostate cancer patient plasma to other cells.

Different studies have suggested the utility of EVs for the identification of prostate cancer-specific biomarkers. However, none of these studies utilized gradient purified exosomes [8,28]. For the first time, we show the presence of αvβ3 integrin in prostate cancer patient serum/plasma exosomes purified through sucrose or iodixanol gradients. We provide evidence that the αvβ3 integrin is found in ExVs shed by prostate epithelial cells in the blood of prostate cancer patients; it is co-expressed with CD9 in PSMA-positive ExVs, and detected at higher levels in ExVs isolated from the blood of prostate cancer patients as compared to age-matched individuals unaffected by this disease or other types of cancer. Furthermore, we demonstrate that CD9 and CD81, both enriched in exosomes [60], are differentially expressed: specifically, CD9 is increased, while CD81 levels are low in ExVs from prostate cancer patients' blood. We also show that β3 is transferred from ExVs isolated from prostate cancer patient plasma to recipient cells in vitro. Our finding that ExVs isolated from the blood of prostate cancer patients show higher levels of the αvβ3 integrin, as compared to ExVs from individuals not affected by cancer, has high relevance for this disease. This is because detection of αvβ3 integrin in the blood, in conjunction with other currently used markers, may meet a need for a more effective noninvasive diagnosis of prostate cancer.

Our group recently showed that exosomes isolated from prostate cancer cells express αvβ6 and αvβ3 and transfer these integrins from prostate cancer cells to other cancer or benign cells [14,20]. Although it has been established that the αvβ3 integrin acts as a receptor for exosome uptake when expressed in recipient cells, such as dendritic cells [63] and hepatic stellate cells [64], the αvβ3 does not appear to play a role in ExV internalization as inhibiting αvβ3 in ExVs through RGD-containing peptides does not decrease or eliminate β3 transfer (as shown in Fig. 3D). The transfer of exosomal αvβ3 integrin may affect intercellular communication, leading to many different outcomes, such as priming a metastatic niche [16,19], altering angiogenesis, overall disease progression and cell signaling [65]. For these properties, the αvβ3 heterodimeric complex needs to be formed; two scenarios may be envisioned: either that αv and β3 present in the exosomes are transferred as a heterodimer or that β3 pairs with av in the recipient cells. Given that αv is expressed in ExVs from patient plasma, the first scenario is more conceivable. In both cases, it is expected that the transfer may also affect cell signaling by altering the levels of other heterodimers in the recipient cells, since αv pairs with many other β subunits.

Ours is the first study to purify exosomes positive for PSMA, a marker up-regulated in prostate cancer, from patient blood. We are the first to describe that αvβ3 in patients' plasma exosomes originates from prostate epithelial cells, as shown in Fig. 4C, where the results show that exosomes are positive for PSMA and express αvβ3 integrin. These PSMA-positive exosomes also express Trop-2. Our lab has previously published that Trop-2, a transmembrane glycoprotein found in prostate cancer cell exosomes, is a novel marker of

capsule-invasive prostate cancer, and functions as a mediator of prostate cancer cell motility and metastasis [66]. Our findings suggest that simultaneous detection of PSMA, αvβ3, and Trop-2 in prostate cancer patient blood exosomes, could fulfill an unmet clinical need for non-invasive diagnostic approaches for prostate cancer. These PSMA-positive ExVs also carry CD9, a tetraspanin known to play a role in protein sorting in exosomes [67], cellular migration and proliferation [68] as well as binding of the αvβ3 integrin in a tertiary complex with JAM-A [69] and other integrins, such as β1 [68,70]. Consistent with our findings, it has been demonstrated thatCD9-positive exosomes are increased in prostate cancer patients compared to patients with BPH [68] and overall, higher levels of plasma CD9 are detected in cancer, such as in acute lymphoblastic leukemia patients [71]. We also show that CD81 expression levels are lower in ExVs from prostate cancer patients compared to ExVs from subjects not affected by cancer. Based on the differential expression of the tetraspaninsCD9 and CD81 in ExVs from subjects not affected by cancer compared to subjects affected by cancer, distinct exosome or ExV populations might arise as cancer initiates and progresses and therefore ExV CD9 and CD81 levels may provide insights into the progression of this disease. Differential expression of CD81, another binding partner of αvβ3 integrin [72], has been demonstrated in other cancers. While higher levels of CD81 are observed in one instance in malignant skin cancer tissues compared to non-melanoma skin cancer tissues, more frequently reduction in expression of CD81 is observed as progression of gastric, hepatocellular or bladder cancer occurs [73–76]. A recent study has shown that CD81 may affect the curvature of the plasma membrane of the cell and cholesterol binding [77]. Since multivesicular bodies containing intraluminal vesicles fuse with the plasma membrane of the cell to be secreted as exosomes into the extracellular space, different levels of CD81 in exosomes from subjects not affected by cancer may affect the exocytotic mechanism that promotes exosome fusion.

Treatments, including chemotherapy, induce changes associated with an aggressive tumor phenotype [78]. Protein cargo composition has been shown to be different in exosomes released by cells that have been treated with a drug compared to exosomes released by non-treated cells [79]. Bandari et al. highlighted that heparanase on the surface of chemotherapy-induced exosomes degrades heparan sulfate embedded within an extracellular matrix [79]. In our study, in contrast, we do not observe a difference in the levels of αvβ3 integrin, CD63, and CD9 in ExVs from prostate cancer patients treated with enzalutamide compared to non-treated cases, thus suggesting that αvβ3 integrin might not be an appropriate marker to monitor response to enzalutamide.

In conclusion, the αvβ3 integrin holds promise as non-invasive biomarker for prostate cancer and, if its role in exosomes has a dominant effect on other pathways, as a potential therapeutic target [65,80]. The utility of blood exosomal αvβ3 integrin as a prognostic as well as a diagnostic marker for prostate cancer will need to be validated in prospective large-scale clinical studies, which also necessitate establishing a simple and rapid detection system.

Experimental procedures

Cell lines

PC3, C4–2B, DU145 and BPH-1 cells and culture conditions have been previously described [14,20].

β3 integrin cDNA constructs

Cloning of β3 integrin cDNA and generation of constructs have been previously described [81]. C4–2B cells expressing β3-GFP were generated in our laboratory using standard transfection protocol using Lipofectamine reagent followed by maintenance of transfectants in complete culture medium containing 5% fetal bovine serum, 1% sodium pyruvate, 1% non-essential amino acids and 1% Penicillin/Streptomycin. Stable transfectants were selected in G418 (1 mg/mL–1.6 mg/mL).

Antibodies and reagents

The following antibodies (Abs) were used for immunoblotting (IB) analysis: mouse monoclonal Abs to PSMA (ab-19,071; Abcam), CD9 (sc-13,118; Santa Cruz Biotechnology), CD81 (ab-23,505; Abcam), CD63 (ab-8219; Abcam), GM130 (61,820; BD Biosciences), EpCAM (2929; Cell Signaling Technology), TUBULIN (T-8535; Sigma); rabbit mAb to TSG101 (ab-125,011; Abcam); rabbit polyclonal Abs (pAbs) to FLOTILLIN1 (FLOT1) (ab-41,927; Abcam), GFP (ab-6556; Abcam), CALNEXIN (CANX) (sc-11,397; Santa Cruz Biotechnology), ERK1 (sc-93; Santa Cruz Biotechnology), and Rb-IgG (Sigma). A goat pAb against human Trop-2 (AF650; R&D Biosystems) was used. A rabbit serum pAb against the cytoplasmic domain of human β3 [51] and a rabbit serum pAb against the cytoplasmic domain of human αv [14] were used. The GRGDSPK peptide (containing an RGD motif) and the GRGESP peptide (containing a RGE motif) were from Gibco Brl. Abiraterone acetate (Janssen Pharmaceuticals) and enzalutamide (Astellas Pharma) were used to treat prostate cancer patients.

Immunoblotting analysis (IB)

IB analysis was performed as previously described [20,82]. The total cell lysates (TCL), ExV lysates or lysates from fractions derived by sucrose and iodixanol gradients were resuspended in RIPA buffer and protein quantification was performed using the BCA assay kit (Pierce). Equal amounts of TCL or ExV lysates were loaded on SDS-PAGE and transferred to PVDF membranes (Millipore). The membranes were blocked in blocking buffers (5% milk in TBS-T or 5% bovine serum albumin (BSA) in TBS-T) followed by incubation with primary and secondary antibodies. Protein expression was detected using chemiluminescence kits from Bioexpress or Thermo Scientific.

ExVs isolation from prostate cancer cells

Isolation of ExVs from PC3, C4–2B Mock, and C4–2B-β3-GFP cells was performed as previously described [14,20,83]. The culture supernatant (SN) was collected after 48 h of serum starvation of cells and processed by differential ultracentrifugation. The SN was first precleared for any dead cells and debris by centrifugation at 2000×*g* for 20 min at 4 °C.

Without disturbing the pellet, the SN was then transferred to a fresh ultracentrifuge tube and centrifuged at 10,000×*g* for 35 min at 4 °C. The remaining SN was then centrifuged to isolate the ExVs at 100,000×*g* for 70 min at 4 °C. The ExVs pellet was further washed in 1×PBS followed by a second centrifugation at 100,000×g for 70 min at 4°C. The final ExVs pellet was resuspended in 1× PBS for storage at –80 °C and subsequent NTA and transfer experiments or lysed in RIPA buffer [14] for IB analysis.

ExV isolation from blood plasma or serum

Blood samples from prostate cancer patients (*n* = 70) and subjects not affected by cancer (*n* = 14) were processed to obtain either serum or plasma. For serum, the blood was allowed to stand at room temperature for 30 min before it was centrifuged at 13,200 rpm for 30 min. To obtain plasma, the blood was added to a tube containing the anti-coagulant EDTA. It was then centrifuged at high speed for 30 min and plasma was collected. A minimum of 3 mL of plasma or serum from patients was used to isolate ExVs by ultracentrifugation. For isolation of ExVs from mice, ~1 mL blood was collected by cardiac puncture in a tube containing Acid Citrate Dextrose (ACD), and ~0.6 mL plasma was collected as described above. A minimum of 0.5 mL of plasma from mice was used to isolate ExVs by ultracentrifugation. ExVs isolation was performed as previously described [84]. Briefly, the serum or plasma samples were pre-cleared by centrifugation at 1500×*g* for 10 min at 4 °C. Without disturbing the pellet, the SN was transferred to a fresh tube and centrifuged at 12,000×*g* for 30 min at 4 °C. The remaining SN was then subjected to centrifugation at 110,000×*g* for 2 h at 4 °C. The ExVs pellet was washed in PBS followed by centrifugation at 110,000×*g* for 2 h at 4 °C. The final ExVs pellet was re-suspended in PBS for storage at –80 °C, NTA, or alternatively lysis buffer was added for IB analysis. ExVs isolation from some serum samples were also performed using Exoquick™ as per the manufacturer's instructions (Systems Biosciences).

Nanoparticle tracking analysis (NTA)

The size distribution analysis for ExVs isolated from the serum and plasma of prostate cancer patients and individuals not affected by cancer was performed as described previously [20,82]. Briefly, ExVs suspensions were diluted 1:1000 and/or 1:200 (for iodixanol purified fractions) in PBS, and the analysis of size distribution and concentration of ExVs was performed, capturing video files of 30-s duration (repeated 3 times) with a frame rate of 30 frames per second of particles moving under Brownian motion using NTA software (NS300, Malvern Instruments). The size distribution and concentration of ExVs from mouse plasma enriched in GFP-tagged αvβ3 integrin were detected utilizing motorized fluorescence filter wheel at 532 nm.

Transmission electron microscopy

The TEM analysis of ExVs purified from prostate cancer patient plasma by differential ultracentrifugation was performed as previously described [14].

Sucrose gradient

ExVs from patient serum (n = 3) were isolated using Exoquick™. The ExVs pellet was resuspended in HEPES/sucrose solution and loaded at the bottom of the tube. A continuous 2 M (bottom) to 0.25 M (top) sucrose gradient was layered on top of the ExVs sample. Steps for the exosome analysis have been previously described [20,83].

Iodixanol gradient

The ExVs isolated from prostate cancer patient plasma (n = 5) by ultracentrifugation were further purified to isolate exosomes, using an iodixanol density gradient centrifugation, modifying a previously published protocol [85]. The 40%, 20%, 10% and 5% wt/vol iodixanol solutions were prepared by diluting a stock solution (60% wt/vol) of Iodixanol (OptiPrep™, Sigma # 1556) with a buffer solution (0.25 M sucrose/ 10 mM Tris, pH 8.0/1 mM EDTA, pH 7.4). The ExVs were mixed with stock iodixanol solution to generate 0.783 mL of 40% iodixanol-ExV suspension and loaded at the bottom of SW55Ti rotor tube (Beckman). Next, 0.783 mLof 20% (wt/vol) iodixanol, 0.783 mL of 10% (wt/vol) iodixanol, and 0.652 mL of 5% (wt/vol) iodixanol were successively layered on top of the 40% iodixanol-ExV suspension to generate a discontinuous iodixanol gradient. The tubes were then centrifuged for 16 h at 100,000×g, 4 °C, in SW55Ti rotor using Beckman, L8–70M Ultracentrifuge. Ten fractions of 275 μL each were then collected starting from the top of the tube. The density of each fraction was assessed with ABBE-3L refractometer (Fisher Scientific). All fractions were diluted and washed with 1 mL PBS and centrifuged for 2 h at 100,000×g, 4°C, in a TLA-100.2 rotor using Beckman, Optima TL Ultracentrifuge. The resulting pellets for each fraction were re-suspended in 30 μL of PBS and stored in –80 °C until further use.

ExV-mediated transfer of αv²3 integrin

BPH-1 and C4–2B cells were serum-starved for 24 h followed by incubation with PC3 ExVs (20 μg/mL, ~10^7 vesicles) for 30 min, or 2, 8, 16, and 24 h. At the end of each time point, cells were trypsinized and then lysed using RIPA buffer. IB analysis was performed to detect β3 expression and the experiment was repeated twice. For β3 transfer via patient plasma ExVs, C4–2B cells were starved for 24 h, incubated with ExVs (30 μg/mL, ~10^8 vesicles) from patient plasma for 24 h and then the cells were trypsinized, lysed and analyzed through IB to detect β3 expression. In both experiments, cells incubated with PBS were used as a negative control (n = 4 biological replicates and 2 technical replicates).

Confocal microscopy

DU145 cells grown on glass cover slips were serum-starved for 24 h followed by incubation for 24 h with (40 pg/ml, ~2 × 10^7 vesicles) or without ExVs isolated from C4–2B-β3-GFP cells. Cells were then washed with PBS (2 washes), fixed with 4% PFA for 15 min at room temperature, washed with PBS (3 washes), quenched with 50 mmol/L NH_4Cl for 15 min, and finally washed with PBS (3 washes). Glass cover slips were mounted on glass slides using ProLong™ diamond antifade mountant with DAPI (Invitrogen). The slides were analyzed and images were captured by Nikon A1R confocal microscope. A Z-stack image

analysis using imaging software NIS Elements Viewer (version 4.11.0) was also performed to evaluate ExV internalization into DU145 cells.

Inhibition of exosomal αv²3 by RGD peptide

PC3 ExVs (~10^7 vesicles) that were pre-treated with either GRGDSPK (RGD) (1 mg/mL) or control GRGESP (RGE) peptide (1 mg/mL) for 1 h at 4 °C, were incubated with BPH-1 or C4–2B cells. After 24 h, cells were lysed in RIPA buffer and β3 levels were determined by IB ($n = 2$).

ExoCap™ EpCAM capture kit

Isolation of EpCAM-positive ExVs was performed using the ExoCap™ EpCAM capture kit (JSR Micro Inc.). PC3 ExVs were isolated using ultracentrifugation and incubated overnight at 4 °C with 100 μL of magnetic beads coated with EpCAM. Samples were processed the following day as per manufacturer's instructions. 1 mL of plasma from six prostate cancer patients was incubated with beads to isolate EpCAM-positive ExVs. PBS was used as negative control while PC3 ExVs were used as positive control. IB was used to analyze the expression levels of β3, EpCAM, and CD9.

Isolation of exosomes by PSMA immunocapture

Rabbit monoclonal antibody to PSMA (ab-133,579, Abcam; 100 μg) or isotype rabbit immunoglobulin (Rb-IgG, 100 μg), each was conjugated with 5 mg of Dynabeads™ M-270 Epoxy beads (Invitrogen) according to the manufacturer's protocol. The antibody-conjugated magnetic beads (~2×10^9 beads/mL) were incubated with iodixanol gradient purified exosomes (~10^9 vesicles) from prostate cancer patients (pooled from $n = 3$) overnight at 4 °C with rotation. After removing unbound exosomes, the bead-exosome complexes were washed with 1 mL PBS, pH 7.4 (3 washes); the immunocaptured whole exosomes were lysed with RIPA buffer, and lysates were collected for IB analysis.

In vivo fluorescence imaging

Ten NSG male mice (10–13 weeks old) were implanted with C4–2B-β3-GFP cells (2×10^6, $n = 6$; 3×10^6, $n = 4$) subcutaneously in their right shoulder and 2×10^6 DU145 cells in their left shoulder. After 5 weeks, mice were euthanized. The excised tissues (C4–2B-β3-GFP right side tumor, DU145 left side tumor, prostates, liver, lungs, seminal vesicles, kidneys, spleen and lymph nodes) were placed on a Petri dish and imaged in an In-Vivo Multispectral FX PRO (MS FX PRO) imaging system (Brucker, Peoria, IL). GFP images were obtained (Ex: 480 nm ± 10 nm, Em: 535 nm ± 10 nm, f-stop 2.8, 4×4 binning, and 5 min exposure) using a cooled charged coupled device (CCD). For anatomical coregistration of fluorescence signal, X-ray images were obtained (f - stop 2.8, 10 s exposure, 4 × 4 binning, and 0.4 mm aluminum filter). For precise co-registration, all images were taken with a 100 mm field of view (FOV) and a focal plane of 17.0 mm. The imaging protocol was approved by institutional IACUC. All mice were maintained under specific pathogen-free conditions. Care and handling of animals was in compliance with IACUC experimental protocols.

Gene expression analysis of CD9 and CD81

Oncomine database was used to compare the expression of CD9 and CD81 between normal and cancerous prostate tissue based on publicly available gene expression data from different prostate cancer studies. For each gene, 4 box plots of expression between cancer and normal samples (2 adenocarcinoma versus normal, 2 carcinoma versus normal) are provided from datasets with the highest number of samples. Supplementary Table S1 contains information about datasets analyzed, type of comparisons made (adenocarcinoma or carcinoma versus normal), number of samples in the datasets and statistical *t*-test *P* value.

Human subject inclusion criteria

The demographics and health information of prostate cancer patients included in this study are listed in Supplementary Table S2. All prostate cancer patients that provided blood samples ($n = 70$) had received a clinical diagnosis of prostate cancer. Patients ranged in age from 18 to 89 years and belonged to two main groups: non-castrate prostate cancer ($n = 41$) and metastatic CRPC ($n = 29$). The non-castrate prostate cancer patients were responsive to bicalutamide or leuprolide at the time blood was obtained and were non-treated with abiraterone acetate or enzalutamide; of these patients, 20 had non-metastatic disease and 21 had metastatic disease. The metastatic CRPC patients received one of two different regimens: 1000 mg of abiraterone acetate daily and prednisone 5 mg twice daily ($n = 16$), or 160 mg enzalutamide daily ($n = 13$). Blood was obtained from castrate-resistant patients at least three weeks after the abiraterone acetate or enzalutamide therapy began. PSA levels were recorded before and after drug treatments. Blood samples were also obtained from age-matched subjects not affected by cancer ($n = 14$). All specimens were de-identified and discarded in accordance with IRB approved protocols.

Supplementary Material

Refer to Web version on PubMed Central for supplementary material.

Acknowledegements

We thank Rachel DeRita, and Dr. Huimin Lu from the Languino laboratory for constructive comments; Dr. Jonathan C.R. Jones from Northwestern University Medical School for generously providing the GFP-β3 integrin cDNA construct; Drs. Tim Manser, Kishore Alugupalli, and Justin Walker for donating NSG mice; Dr. Michael Root laboratory for providing access to refractometer; Dr. Karen Bussard, Dr. Marco Trerotola for insightful discussion; Dr. Mark Fortini and Jennifer Wilson fortechnical writing comments; Dr. James Keen and Yolanda Covarrubias, bio-imaging facility, for technical support in imaging; Dr. Jianke Zhang and Amir Yarmahmoodi, flow cytometry facility for technical support in NTA experiments; and Veronica Robles for administrative assistance.

Funding information

This study was supported by NIH R01 CA109874, P01 CA140043 (to L.R.L), NIH/NCI RO1 157372 (to M.L.T.), NIH RO1 CA39481, RO1 CA47282 (to R.V·I). This project was also funded, in part, under a Commonwealth University Research Enhancement Program grant with the Pennsylvania Department of Health (H.R.); the Department specifically disclaims responsibility for any analyses, interpretations or conclusions. The Sidney Kimmel Cancer Center flow cytometry facility and bio-imaging facility are supported by the NCI, National Institutes of Health, under award P30CA056036.

References

[1]. Siegel RL, Miller KD, Jemal A, Cancer statistics, 2018, CA Cancer J. Clin. 68 (1) (2018) 7–30. [PubMed: 29313949]

[2]. Mitchell T, Neal DE, The genomic evolution of human prostate cancer, Br. J. Cancer 113 (2) (2015) 193–198. [PubMed: 26125442]

[3]. Culig Z, Targeting the androgen receptor in prostate cancer, Expert. Opin. Pharmacother. 15 (10) (2014) 1427–1437. [PubMed: 24890318]

[4]. Isaacs JT, The biology of hormone refractory prostate cancer. Why does it develop? Urol. Clin. North Am. 26 (2) (1999) 263–273. [PubMed: 10361549]

[5]. Beer TM, Armstrong AJ, Rathkopf DE, Loriot Y, Sternberg CN, Higano CS, Iversen P, Bhattacharya S, Carles J, Chowdhury S, Davis ID, de Bono JS, Evans CP, Fizazi K, Joshua AM, Kim CS, Kimura G, Mainwaring P, Mansbach H, Miller K, Noonberg SB, Perabo F, Phung D, Saad F, Scher HI, Taplin ME, Venner PM, Tombal B, Enzalutamide in metastatic prostate cancer before chemotherapy, N. Engl. J. Med. 371 (5) (2014) 424–433. [PubMed: 24881730]

[6]. de Bono JS, Logothetis CJ, Molina A, Fizazi K, North S, Chu L, Chi KN, Jones RJ, Goodman OB Jr.,Saad F, Staffurth JN, Mainwaring P, Harland S, Flaig TW, Hutson TE, Cheng T, Patterson H, Hainsworth JD, Ryan CJ, Sternberg CN, Ellard SL, Flechon A, Saleh M, Scholz M, Efstathiou E, Zivi A, Bianchini D, Loriot Y, Chieffo N, Kheoh T, Haqq CM, Scher HI, Abiraterone and increased survival in metastatic prostate cancer, N. Engl. J. Med. 364 (21) (2011) 1995–2005. [PubMed: 21612468]

[7]. Velonas VM, Woo HH, dos Remedios CG, Assinder SJ, Current status of biomarkers for prostate cancer, Int. J. Mol. Sci. 14 (6) (2013) 11034–11060. [PubMed: 23708103]

[8]. Khan S, Jutzy JM, Valenzuela MM, Turay D, Aspe JR, Ashok A, Mirshahidi S, Mercola D, Lilly MB, Wall NR, Plasma-derived exosomal survivin, a plausible biomarker for early detection of prostate cancer, PLoS One 7 (10) (2012) e46737.

[9]. Li Y, Zhang Y, Qiu F, Qiu Z, Proteomic identification of exosomal LRG1: a potential urinary biomarker for detecting NSCLC, Electrophoresis 32 (15) (2011) 1976–1983. [PubMed: 21557262]

[10]. Melo SA, Luecke LB, Kahlert C, Fernandez AF, Gammon ST, Kaye J, Lebleu VS, Mittendorf EA, Weitz J, Rahbari N, Reissfelder C, Pilarsky C, Fraga MF, Piwnica-Worms D, Kalluri R, Glypican-1 identifies cancer exosomes and detects early pancreatic cancer, Nature 523 (7559) (2015) 177–182. [PubMed: 26106858]

[11]. Skog J, Wurdinger T, van Rijn S, Meijer DH, Gainche L, Sena-Esteves M, Curry WT Jr., B.S. Carter, A.M. Krichevsky, X.O. Breakefield, Glioblastoma microvesicles transport RNA and proteins that promote tumour growth and provide diagnostic biomarkers, Nat. Cell Biol. 10 (12) (2008) 1470–1476. [PubMed: 19011622]

[12]. Tanaka Y, Kamohara H, Kinoshita K, Kurashige J, Ishimoto T, Iwatsuki M, Watanabe M, Baba H, Clinical impact of serum exosomal microRNA-21 as a clinical biomarker in human esophageal squamous cell carcinoma, Cancer 119 (6) (2013) 1159–1167. [PubMed: 23224754]

[13]. Taylor DD, Gercel-Taylor C, MicroRNA signatures of tumor-derived exosomes as diagnostic biomarkers of ovarian cancer, Gynecol. Oncol. 110 (1) (2008) 13–21. [PubMed: 18589210]

[14]. Fedele C, Singh A, Zerlanko BJ, Iozzo RV, Languino LR, The αvβ6 integrin is transferred intercellularly via exosomes, J. Biol. Chem. 290 (8) (2015) 4545–4551. [PubMed: 25568317]

[15]. He M, Qin H, Poon TC, Sze SC, Ding X, Co NN, Ngai SM, Chan TF, Wong N, Hepatocellular carcinoma-derived exosomes promote motility of immortalized hepatocyte through transfer of oncogenic proteins and RNAs, Carcinogenesis 36 (9) (2015) 1008–1018. [PubMed: 26054723]

[16]. Hoshino A, Costa-Silva B, Shen TL, Rodrigues G, Hashimoto A, Tesic Mark M, Molina H, Kohsaka S, Di Giannatale A, Ceder S, Singh S, Williams C, Soplop N, Uryu K, Pharmer L, King T, Bojmar L, Davies AE, Ararso Y, Zhang T, Zhang H, Hernandez J, Weiss JM, Dumont-Cole VD, Kramer K, Wexler LH, Narendran A, Schwartz GK, Healey JH, Sandstrom P, Jorgen Labori K, Kure EH, Grandgenett PM, Hollingsworth MA, de Sousa M, Kaur S, Jain M, Mallya K, Batra SK, Jarnagin WR, Brady MS, Fodstad O, Muller V, Pantel K, Minn AJ, Bissell MJ, Garcia BA, Kang Y, Rajasekhar VK, Ghajar CM, Matei I, Peinado H, Bromberg J, Lyden D, Tumour

exosome integrins determine organotropic metastasis, Nature 527 (7578) (2015) 329–335. [PubMed: 26524530]

[17]. Hosseini-Beheshti E, Choi W, Weiswald LB, Kharmate G, Ghaffari M, Roshan-Moniri M, Hassona MD, Chan L, Chin MY, Tai IT, Rennie PS, Fazli L, Tomlinson Guns ES, Exosomes confer pro-survival signals to alter the phenotype of prostate cells in their surrounding environment, Oncotarget 7 (2016) 14639–14658. [PubMed: 26840259]

[18]. McAtee CO, Booth C, Elowsky C, Zhao L, Payne J, Fangman T, Caplan S, Henry MD, Simpson MA, Prostate tumor cell exosomes containing hyaluronidase Hyal1 stimulate prostate stromal cell motility by engagement of FAK-mediated integrin signaling, Matrix Biol. (2018)10.1016/j.matbio.2018.05.002.

[19]. Peinado H, Aleckovic M, Lavotshkin S, Matei I, Costa-Silva B, Moreno-Bueno G, Hergueta-Redondo M, Williams C, Garcia-Santos G, Ghajar C, Nitadori-Hoshino A, Hoffman C, Badal K, Garcia BA, Callahan MK, Yuan J, Martins VR, Skog J, Kaplan RN, Brady MS, Wolchok JD, Chapman PB, Kang Y, Bromberg J, Lyden D, Melanoma exosomes educate bone marrow progenitor cells toward a pro-metastatic phenotype through MET, Nat. Med. 18 (6) (2012) 883–891. [PubMed: 22635005]

[20]. Singh A, Fedele C, Lu H, Nevalainen MT, Keen JH, Languino LR, Exosome-mediated transfer of αvβ3 integrin from tumorigenic to non-tumorigenic cells promotes a migratory phenotype, Mol. Cancer Res. 14 (11) (2016) 1136–1146. [PubMed: 27439335]

[21]. Soekmadji C, Russell PJ, Nelson CC, Exosomes in prostate cancer: putting together the pieces of a puzzle, Cancers (Basel) 5 (4) (2013) 1522–1544. [PubMed: 24351670]

[22]. Kawakami K, Fujita Y, Matsuda Y, Arai T, Horie K, Kameyama K, Kato T, Masunaga K, Kasuya Y, Tanaka M, Mizutani K, Deguchi T, Ito M, Gamma-glutamyltransferase activity in exosomes as a potential marker for prostate cancer, BMC Cancer 17 (1) (2017) 316. [PubMed: 28476099]

[23]. Soekmadji C, Corcoran NM, Oleinikova I, Jovanovic L, Ramm GA, Nelson CC, Jenster G, Russell PJ, Extracellular vesicles for personalized therapy decision support in advanced metastatic cancers and its potential impact for prostate cancer, Prostate 77 (14) (2017) 1416–1423. [PubMed: 28856701]

[24]. Valentino A, Reclusa P, Sirera R, Giallombardo M, Camps C, Pauwels P, Crispi S, Rolfo C, Exosomal micro-RNAs in liquid biopsies: future biomarkers for prostate cancer, Clin. Transl. Oncol. 19 (6) (2017) 651–657. [PubMed: 28054319]

[25]. Huang X, Yuan T, Liang M, Du M, Xia S, Dittmar R, Wang D, See W, Costello BA, Quevedo F, Tan W, Nandy D, Bevan GH, Longenbach S, Sun Z, Lu Y, Wang T, Thibodeau S, Boardman L, Kohli M, Wang L, Exosomal miR-1290 and miR-375 as prognostic markers in castration-resistant prostate cancer, Eur. Urol. 1 (2015)33–41.

[26]. Wang YH, Ji J, Wang BC, Chen H, Yang ZH, Wang K, Luo CL, Zhang WW, Wang FB, Zhang XL, Tumor-derived exosomal long noncoding RNAs as promising diagnostic biomarkers for prostate cancer, Cell. Physiol. Biochem. 46 (2) (2018) 532–545. [PubMed: 29614511]

[27]. Kharmate G, Hosseini-Beheshti E, Caradec J, Chin MY, Tomlinson Guns ES, Epidermal growth factor receptor in prostate cancer derived exosomes, PLoS One 11 (5) (2016), e0154967.

[28]. Logozzi M, Angelini DF, lessi E, Mizzoni D, Di Raimo R, Federici C, Lugini L, Borsellino G, Gentilucci A, Pierella F, Marzio V, Sciarra A, Battistini L, Fais S, Increased PSA expression on prostate cancer exosomes in in vitro condition and in cancer patients, Cancer Lett. 403 (Sep 10) (2017) 318–329. [PubMed: 28694142]

[29]. Di Vizio D, Morello M, Dudley AC, Schow PW, Adam RM, Morley S, Mulholland D, Rotinen M, Hager MH, Insabato L, Moses MA, Demichelis F, Lisanti MP, Wu H, Klagsbrun M, Bhowmick NA, Rubin MA, D'Souza-Schorey C, Freeman MR, Large oncosomes in human prostate cancer tissues and in the circulation of mice with metastatic disease, Am. J. Pathol. 181 (5) (2012) 1573–1584. [PubMed: 23022210]

[30]. Minciacchi VR, You S, Spinelli C, Morley S, Zandian M, Aspuria PJ, Cavallini L, Ciardiello C, Reis Sobreiro M, Morello M, Kharmate G, Jang SC, Kim DK, Hosseini-Beheshti E, Tomlinson Guns E, Gleave M, Gho YS, Mathivanan S, Yang W, Freeman MR, Di Vizio D, Large oncosomes contain distinct protein cargo and represent a separate functional class of tumor-derived extracellular vesicles, Oncotarget 6 (13) (2015) 11327–11341. [PubMed: 25857301]

[31]. Ristau B, O'Keefe D, Bacich D, The prostate-specific membrane antigen: lessons and current clinical implications from 20 years of research, Urol. Oncol. 32 (3) (2014) 272–279. [PubMed: 24321253]

[32]. Mizutani K, Terazawa R, Kameyama K, Kato T, Horie K, Tsuchiya T, Seike K, Ehara H, Fujita Y, Kawakami K, Ito M, Deguchi T, Isolation of prostate cancer-related exosomes, Anticancer Res. 34 (7) (2014) 3419–3423. [PubMed: 24982349]

[33]. Nauroy P, Hughes S, Naba A, Ruggiero F, The in-silico zebrafish matrisome: a new tool to study extracellular matrix gene and protein functions, Matrix Biol. 65 (2018) 5–13. [PubMed: 28739138]

[34]. Gubbiotti MA,Neill T, Iozzo RV, A current view of perlecan in physiology and pathology: a mosaic of functions, Matrix Biol. 57–58 (2017) 285–298.

[35]. Li S, Qi Y, McKee K, Liu J, Hsu J, Yurchenco PD, Integrin and dystroglycan compensate each other to mediate laminin-dependent basement membrane assembly and epiblast polarization, Matrix Biol. 57–58 (2017) 272–284.

[36]. Miller RT, Mechanical properties of basement membrane in health and disease, Matrix Biol. 57–58 (2017) 366–373.

[37]. Pozzi A, Yurchenco PD, lozzo RV, The nature and biology of basement membranes, Matrix Biol. 57–58 (2017) 1–11.

[38]. Randles MJ, Humphries MJ, Lennon R, Proteomic definitions of basement membrane composition in health and disease, Matrix Biol. 57–58 (2017) 12–28.

[39]. Hui T, Sorensen ES, Rittling SR, Osteopontin binding to the alpha 4 integrin requires highest affinity integrin conformation, but is independent of post-translational modifications of osteopontin, Matrix Biol. 41 (2015) 19–25. [PubMed: 25446551]

[40]. Roche F, Sipila K, Honjo S, Johansson S, Tugues S, Heino J, Claesson-Welsh L, Histidine-rich glycoprotein blocks collagen-binding integrins and adhesion of endothelial cells through low-affinity interaction with a2 integrin, Matrix Biol. 48 (2015) 89–99. [PubMed: 26051322]

[41]. Shinde AV, Kelsh R, Peters JH, Sekiguchi K, van De Water L, McKeown-Longo PJ, The a4ß1 integrin and the EDA domain of fibronectin regulate a profibrotic phenotype in dermal fibroblasts, Matrix Biol. 41 (2015) 26–35. [PubMed: 25433338]

[42]. Twal WO, Hammad SM, Guffy SL, Argraves WS, A novel intracellular fibulin-1D variant binds to the cytoplasmic domain of integrin beta1 subunit, Matrix Biol. 43 (2015) 97–108. [PubMed: 25661773]

[43]. Viquez OM, Yazlovitskaya EM, Tu T, Mernaugh G, Secades P, McKee KK, Georges-Labouesse E, De Arcangelis A, Quaranta V, Yurchenco P, Gewin LC, Sonnenberg A, Pozzi A, Zent R, Integrin alpha6 maintains the structural integrity of the kidney collecting system, Matrix Biol. 57–58 (2017) 244–257.

[44]. Felding-Habermann B, Integrin adhesion receptors in tumor metastasis, Clin. Exp. Metastasis 20 (3) (2003) 203–213. [PubMed: 12741679]

[45]. Fornaro M, Manes T, Languino LR, Integrins and prostate cancer metastases, Cancer Metastasis Rev. 20 (3–4) (2001) 321–331. [PubMed: 12085969]

[46]. Hamidi H, Pietila M, Ivaska J, The complexity of integrins in cancer and new scopes for therapeutic targeting, Br. J. Cancer 115 (9) (2016) 1017–1023. [PubMed: 27685444]

[47]. Drivalos A, Chrisofos M, Efstathiou E, Kapranou A, Kollaitis G, Koutlis G, Antoniou N, Karanastasis D, Dimopoulos MA, Bamias A, Expression of a5-integrin, a7-integrin, E-cadherin, and N-cadherin in localized prostate cancer, Urol. Oncol. 34 (4) (2016).

[48]. Goel HL, Li J, Kogan S, Languino LR, Integrins in prostate cancer progression, Endocr. Relat. Cancer 15 (3) (2008) 657–664. [PubMed: 18524948]

[49]. Lu H, Wang T, Li J, Fedele C, Liu Q, Zhang J, Jiang Z, Jain D, Iozzo RV, Violette SM, Weinreb PH, Davis RJ, Gioeli D, Fitzgerald TJ, Altieri DC, Languino LR, avß6 integrin promotes castrate-resistant prostate cancer through JNK1-mediated activation of androgen receptor, Cancer Res. 1 (76) (2016) 5163–5174.

[50]. Cress AE, Rabinovitz I, Zhu W, Nagle RB, The α6β1 and α6β4 integrins in human prostate cancer progression, Cancer Metastasis Rev. 14 (3) (1995) 219–228. [PubMed: 8548870]

[51]. Zheng DQ, Woodard AS, Fornaro M, Tallini G, Languino LR, Prostatic carcinoma cell migration via αvβ3 integrin is modulated by a focal adhesion kinase pathway, Cancer Res. 59 (7) (1999) 1655–1664. [PubMed: 10197643]

[52]. Stucci S, Tucci M, Passarelli A, Silvestris F, αvβ3 integrin: Pathogenetic role in osteotropic tumors, Crit. Rev. Oncol. Hematol. 96 (1) (2015) 183–193. [PubMed: 26126493]

[53]. McCabe NP, De S, Vasanji A, Brainard J, Byzova TV, Prostate cancer specific integrin alphavbeta3 modulates bone metastatic growth and tissue remodeling, Oncogene 26 (42) (2007) 6238–6243. [PubMed: 17369840]

[54]. Chen Y, Lee H, Tong H, Schwartz M, Zhu C, Force regulated conformational change of integrin αvβ3, Matrix Biol. 60–61 (2017) 70–85.

[55]. Brauchle E, Kasper J, Daum R, Schierbaum N, Falch C, Kirschniak A, Schäffer TE, Schenke-Layland K, Biomechanical and biomolecular characterization of extra-cellular matrix structures in human colon carcinomas, Matrix Biol. 68–69 (2018) 180–193.

[56]. Ringer P, Colo G, Fässler R, Grashoff C, Sensing the mechano-chemical properties of the extracellular matrix, Matrix Biol. 64 (2017) 6–16. [PubMed: 28389162]

[57]. Bijnsdorp IV, Geldof AA, Lavaei M, Piersma SR, van Moorselaar RJ, Jimenez CR, Exosomal ITGA3 interferes with non-cancerous prostate cell functions and is increased in urine exosomes of metastatic prostate cancer patients, J. Extracell. Vesicles 2 (1) (2013) 22097.

[58]. Lu H, Bowler N, Harshyne LA, Hooper DC, Krishn SR, Kurtoglu S, Fedele C, Liu Q, Tang HY, Kossenkov AV, Kelly WK, Wang K, Kean RB, Weinreb PH, Yu L, Dutta A, Fortina P, Ertel A, Gabrilovich DI, Speicher DW, Altieri DC, Languino LR, Exosomal avß6 integrin is required for monocyte M2 polarization in prostate cancer, Matrix Biol. 70 (2018) 20–35. [PubMed: 29530483]

[59]. Colombo M, Raposo G, Thery C, Biogenesis, secretion, and intercellular interactions of exosomes and other extra-cellular vesicles, Annu. Rev. Cell Dev. Biol. 30 (2014) 255–289. [PubMed: 25288114]

[60]. Kowal J, Arras G, Colombo M, Jouve M, Morath JP, Primdal-Bengtson B, Dingli F, Loew D, Tkach M, Thery C, Proteomic comparison defines novel markers to characterize heterogeneous populations of extracellular vesicle subtypes, Proc. Natl. Acad. Sci. U. S. A. 113 (8) (2016) E968–E977. [PubMed: 26858453]

[61]. Sanderson RD, Bandari SK, Vlodavsky I, Proteases and glycosidases on the surface of exosomes: newly discovered mechanisms for extracellular remodeling, Matrix Biol. 17 (2017) 30311–30316.

[62]. Hayward SW, Cunha GR, Bartek J, Deshpande N, Narayan P, Establishment and characterization of an immortalized but not transformed human prostate epithelial cell line: BPH-1, In Vitro Cell. Dev. Biol. Anim. 31 (1995) 14–24.

[63]. Morelli AE, Larregina AT, Shufesky WJ, Sullivan ML, Stolz DB, Papworth GD, Zahorchak AF, Logar AJ, Wang Z, Watkins SC, Falo LD Jr., A.W. Thomson, Endocytosis, intracellular sorting, and processing of exosomes by dendritic cells, Blood 104 (10) (2004) 3257–3266. [PubMed: 15284116]

[64]. Chen L, Brigstock DR, Integrins and heparan sulfate proteoglycans on hepatic stellate cells (HSC) are novel receptors for HSC-derived exosomes, FEBS Lett. 590 (2016) 4263–4274. [PubMed: 27714787]

[65]. Junker K, Heinzelmann J, Beckham C, Ochiya T, Jenster G, Extracellular vesicles and their role in urologic malignancies, Eur. Urol. 70 (2) (2016) 323–331. [PubMed: 26924769]

[66]. Trerotola M, Ganguly KK, Fazli L, Fedele C, Lu H, Dutta A, Liu Q, De Angelis T, Riddell LW, Riobo NA, Gleave ME, Zoubeidi A, Pestell RG, Altieri DC, Languino LR, Trop-2 is up-regulated in invasive prostate cancer and displaces FAK from focal contacts, Oncotarget 6 (16) (2015) 14318–14328. [PubMed: 26015409]

[67]. Andreu Z, Yanez-Mo M, Tetraspanins in extracellular vesicle formation and function, Front. Immunol. 5 (2014) 442. [PubMed: 25278937]

[68]. Soekmadji C, Riches JD, Russell PJ, Ruelcke JE, McPherson S, Wang C, Hovens CM, Corcoran NM, The Australian Prostate Cancer Collaboration, Hill MM, Nelson CC, Modulation of

paracrine signaling by CD9 positive small extracellular vesicles mediates cellular growth of androgen deprived prostate cancer, Oncotarget 8 (32) (2016) 52237–52255. [PubMed: 28881726]

[69]. Peddibhotla SS, Brinkmann BF, Kummer D, Tuncay H, Nakayama M, Adams RH, Gerke V, Ebnet K, Tetraspanin CD9 links junctional adhesion molecule-Ato αvβ3 integrin to mediate basic fibroblast growth factor-specific angiogenic signaling, Mol. Biol. Cell 24 (7) (2013) 933–944. [PubMed: 23389628]

[70]. Murayama Y, Shinomura Y, Oritani K, Miyagawa J, Yoshida H, Nishida M, Katsube F, Shiraga M, Miyazaki T, Nakamoto T, Tsutsui S, Tamura S, Higashiyama S, Shimomura I, Hayashi N, The tetraspanin CD9 modulates epidermal growth factor receptor signaling in cancer cells, J. Cell. Physiol. 216 (1) (2008) 135–143. [PubMed: 18247373]

[71]. Komada Y, Peiper SC, Melvin SL, Tarnowski B, Green AA, A monoclonal antibody (SJ-9A4) to P24 present on common alls, neuroblastomas and platelets - ii. Characterization of P24 and shedding in vitro and in vivo, Leuk. Res. 7 (4) (1983) 499–507. [PubMed: 6578391]

[72]. Yu J, Lee CY, Changou CA, Cedano-Prieto DM, Takada YK, Takada Y, The CD9, CD81, and CD151 EC2 domains bind to the classical rgd-binding site of integrin avß3, Biochem. J. 474 (4) (2017) 589–596. [PubMed: 27993971]

[73]. Hong IK, Byun HJ, Lee J, Jin YJ, Wang SJ, Jeoung DI, Kim YM, Lee H, The tetraspanin CD81 protein increases melanoma cell motility by up-regulating metalloproteinase MT1-MMP expression through the pro-oncogenic AKT-dependent Sp1 activation signaling pathways, J. Biol. Chem. 289 (22) (2014) 15691–15704. [PubMed: 24733393]

[74]. Yoo TH, Ryu BK, Lee MG, Chi SG, CD81 is a candidate tumor suppressor gene in human gastric cancer, Cell Oncol. (Dordr). 36 (2) (2013) 141–153. [PubMed: 23264205]

[75]. Inoue G, Horiike N, Onji M, The CD81 expression in liver in hepatocellular carcinoma, Int. J. Mol. Med. 7 (1) (2001) 67–71. [PubMed: 11115611]

[76]. Lee MS, Kim JH, Lee JS, Yun SJ, Kim WJ, Ahn H, Park J, Prognostic significance of creb-binding protein and CD81 expression in primary high grade non-muscle invasive bladder cancer: Identification of novel biomarkers for bladder cancer using antibody microarray, PLoS One 10 (4) (2015), e0125405.

[77]. Zimmerman B, Kelly B, McMillan BJ, Seegar TC, Dror RO, Kruse AC, Blacklow SC, Crystal structure of a full-length human tetraspanin reveals a cholesterol-binding pocket, Cell 167 (4) (2016) 1041–1051. [PubMed: 27881302]

[78]. Ramani V, Vlodavsky I, Ng M, Zhang Y, Barbieri P, Noseda A, Sanderson R, Chemotherapy induces expression and release of heparanase leading to changes associated with an aggressive tumor phenotype, Matrix Biol. 55 (2016) 22–34. [PubMed: 27016342]

[79]. Bandari SK, Purushothaman A, Ramani VC, Brinkley GJ, Chandrashekar DS, Varambally S, Mobley JA, Zhang Y, Brown EE, Vlodavsky I, Sanderson RD, Chemotherapy induces secretion of exosomes loaded with heparanase that degrades extracellular matrix and impacts tumor and host cell behavior, Matrix Biol. 65 (2018) 104–118. [PubMed: 28888912]

[80]. Verma M, Lam TK, Hebert E, Divi RL, Extracellular vesicles: potential applications in cancer diagnosis, prognosis, and epidemiology, BMC Clin. Pathol. 15 (2015) 6. [PubMed: 25883534]

[81]. Tsuruta D, Gonzales M, Hopkinson SB, Otey C, Khuon S, Goldman RD, Jones JC, Microfilament-dependent movement of the β3 integrin subunit within focal contacts of endothelial cells, FASEB J. 16 (8) (2002) 866–868. [PubMed: 11967230]

[82]. Derita RM, Zerlanko B, Singh A, Lu H, Iozzo RV, Benovic JL, Languino LR, c-Src, insulin-like growth factor I receptor, G-protein-coupled receptor kinases and focal adhesion kinase are enriched into prostate cancer cell exosomes, J. Cell. Biochem. 118 (1) (2017) 66–73. [PubMed: 27232975]

[83]. Thery C, Amigorena S, Raposo G, Clayton A, Isolation and characterization of exosomes from cell culture supernatants and biological fluids, Curr. Protoc. Cell Biol. (2006) 3.22.1–3.22.29.

[84]. Kharaziha P, Chioureas D, Rutishauser D, Baltatzis G, Lennartsson L, Fonseca P, Azimi A, Hultenby K, Zubarev R, Ullen A, Yachnin J, Nilsson S, Panaretakis T, Molecular profiling of prostate cancer derived exosomes may reveal a predictive signature for response to docetaxel, Oncotarget 6 (25) (2015) 21740–21754. [PubMed: 25844599]

[85]. Lobb RJ, Becker M, Wen SW, Wong CS, Wiegmans AP, Leimgruber A, Moller A, Optimized exosome isolation protocol for cell culture supernatant and human plasma, J. Extracell. Vesicles. 4 (2015) 27031. [PubMed: 26194179]

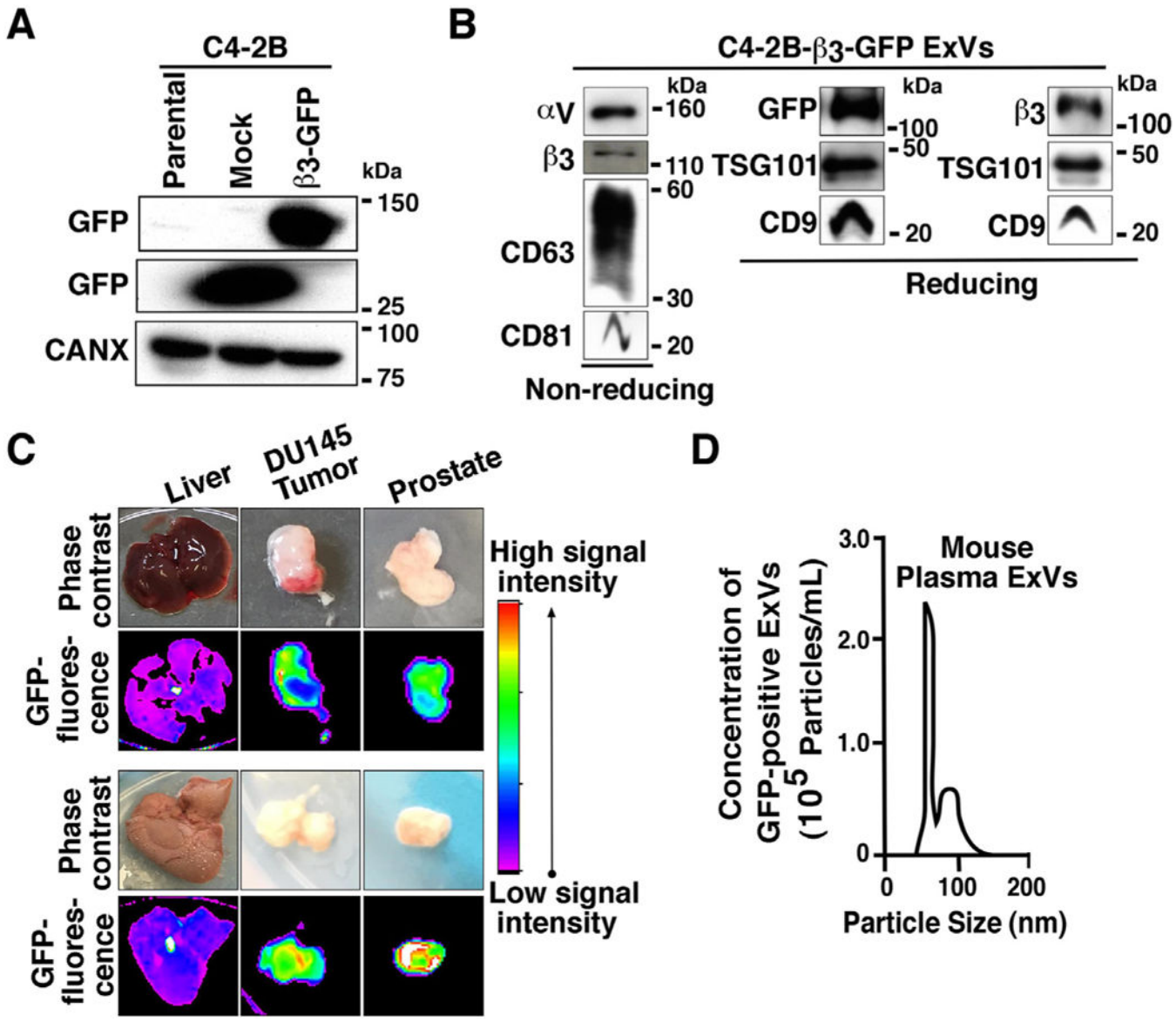

Fig. 1.

GFP-tagged αvβ3 integrin is expressed in prostate cancer cell ExVs, and it is localized in distant lesions in vivo. (A) IB analysis of expression of GFP in total cell lysates (TCL) from parental C4-2B, C4-2B-GFP (Mock) and C4-2B-β3-GFP cells. Calnexin (CANX) was used as loading control. (B) IB analysis of expression of αv, β3, CD63, CD81 (non-reducing conditions) and GFP, β3, TSG101, CD9 (reducing conditions) in lysates from ExVs derived from C4-2B-β3-GFP cells by differential ultracentrifugation. (C) In vivo fluorescence and corresponding phase contrast images are shown for liver, DU145 tumor, and prostate isolated from NSG mice that were injected subcutaneously with C4-2B-β3-GFP cells on the right side and non-transfected DU145 cells on the left side. Two representative samples are shown. (D) NTA for size distribution and concentration of GFP-positive ExVs isolated by differential ultracentrifugation from plasma of the mice subcutaneously injected with C4-2B-β3-GFP cells. One representative sample is shown.

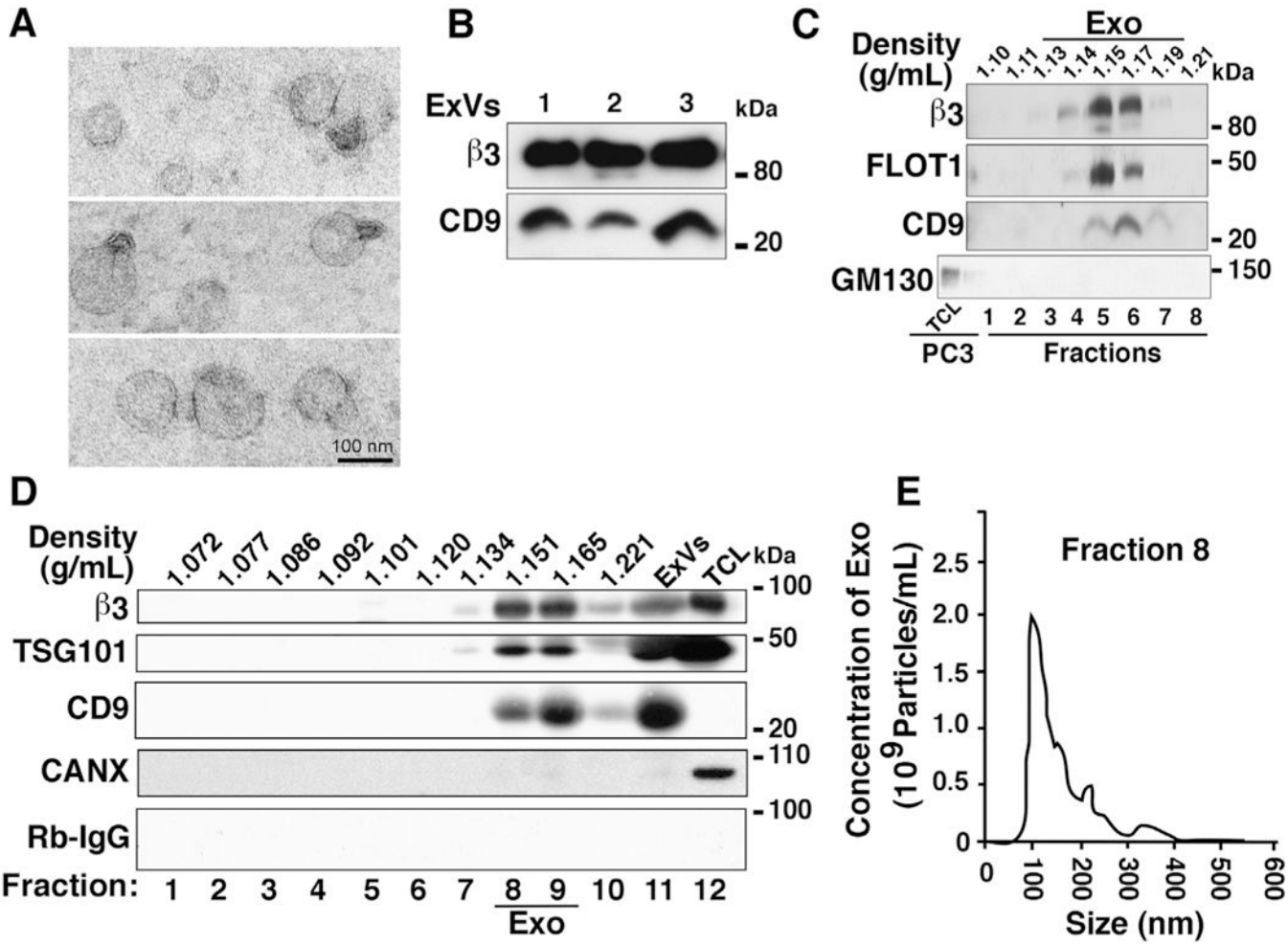

Fig. 2.

Expression of αvβ3 integrin in exosomes derived from plasma of prostate cancer patients. (A) Transmission electron microscopy (TEM) of negatively stained ExVs isolated from prostate cancer patient plasma by differential ultracentrifugation. Scale bar = 100 nm. (B) IB analysis for expression of p3 integrin and exosomal marker CD9 in lysates from ExVs purified from prostate cancer patient plasma by differential ultracentrifugation. The results from three representative samples are shown. (C) Sucrose gradient analysis of ExVs isolated from prostate cancer patient serum using Exoquick™. Expression of β3 integrin and exosomal markers FLOT1 and CD9 in eight different fractions is shown. GM130 (cis-Golgi marker) is expressed in PC3 lysate (TCL) and is absent in all fractions. The density at which exosomes float in sucrose gradient is between 1.13 and 1.19 g/mL. (D) IB analysis for expression of β3 integrin in ten fractions derived from iodixanol gradient centrifugation of ExVs isolated by differential ultracentrifugation of prostate cancer patient plasma. Expression of TSG101 and CD9 was analyzed as markers present in exosomes, Calnexin (CANX) was analyzed as a marker absent in exosomes, while Rabbit IgG (Rb-IgG) was used as a negative control for β3. ExV lysate derived by ultracentrifugation was used as input and PC3 lysate (TCL) was used as positive control for expression of β3, TSG101, and

CANX. (E) NTA for size distribution and concentration of purified exosomes (Exo) in fraction eight (Density = 1.151 g/mL) from iodixanol density gradient.

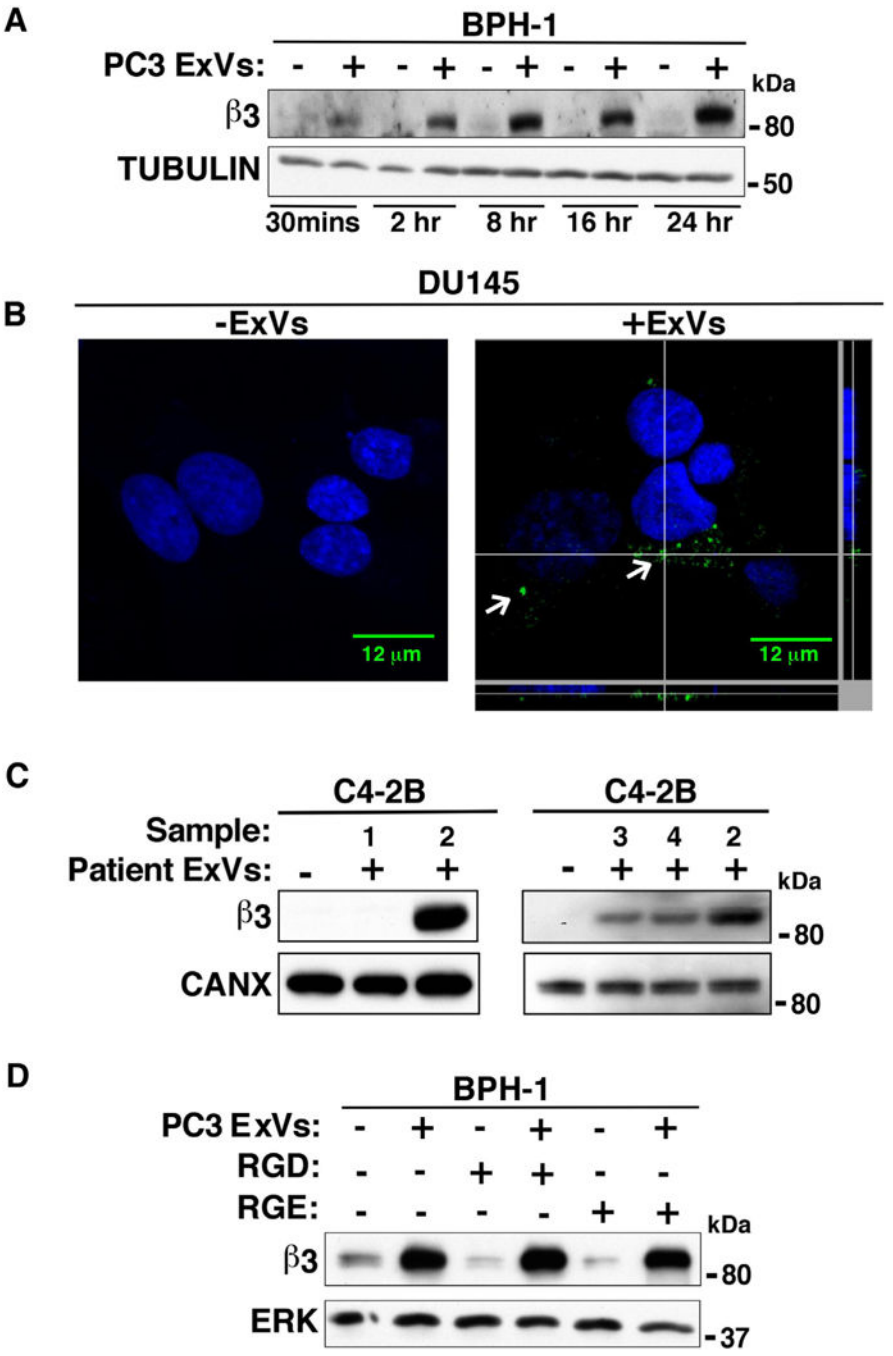

Fig. 3.

ExVs mediate transfer of αvβ3 integrin to recipient cells. (A) IB analysis shows β3 expression levels in BPH-1 cells incubated with PC3-derived ExVs (+) at different time points (30 min to 24 h). BPH-1 cells treated with PBS alone (–) are used as a negative control. TUBULIN expression is included as loading control. (B) DU145 cells were incubated with ExVs (40 μg/ml, right) derived from C4–2B-β3-GFP cells or vehicle alone (left) for 24 h. An intracellular green fluorescent signal corresponding to ExV mediated internalization of β3-GFP was evaluated by confocal microscopy. DAPI was used to detect

cell nuclei (blue). Scale bar = 12 μm. The GFP signal corresponding to ExV mediated internalization of β3-GFP in DU145 cells is shown (white arrows). *Z*-stack analysis shows the intracellular GFP signal in a cell. (C) ExVs were isolated from the plasma of 4 patients (designated 1, 2, 3 and 4) by ultracentrifugation and incubated with C4–2B cells. After 24 h, IB was used to analyze β3 integrin expression levels. C4–2B cells treated with vehicle alone are used as a negative control. CANX serves as loading control. (D) PC3-derived ExVs pre-treated with GRGDSPK peptide (1 mg/mL) for 1 h at 4 °C were incubated with serum-starved BPH-1 cells for 24 h followed by IB analysis to measure β3 levels. BPH-1 cells incubated with GRGESP (1 mg/mL) are used as a negative control. ERK is used as loading control.

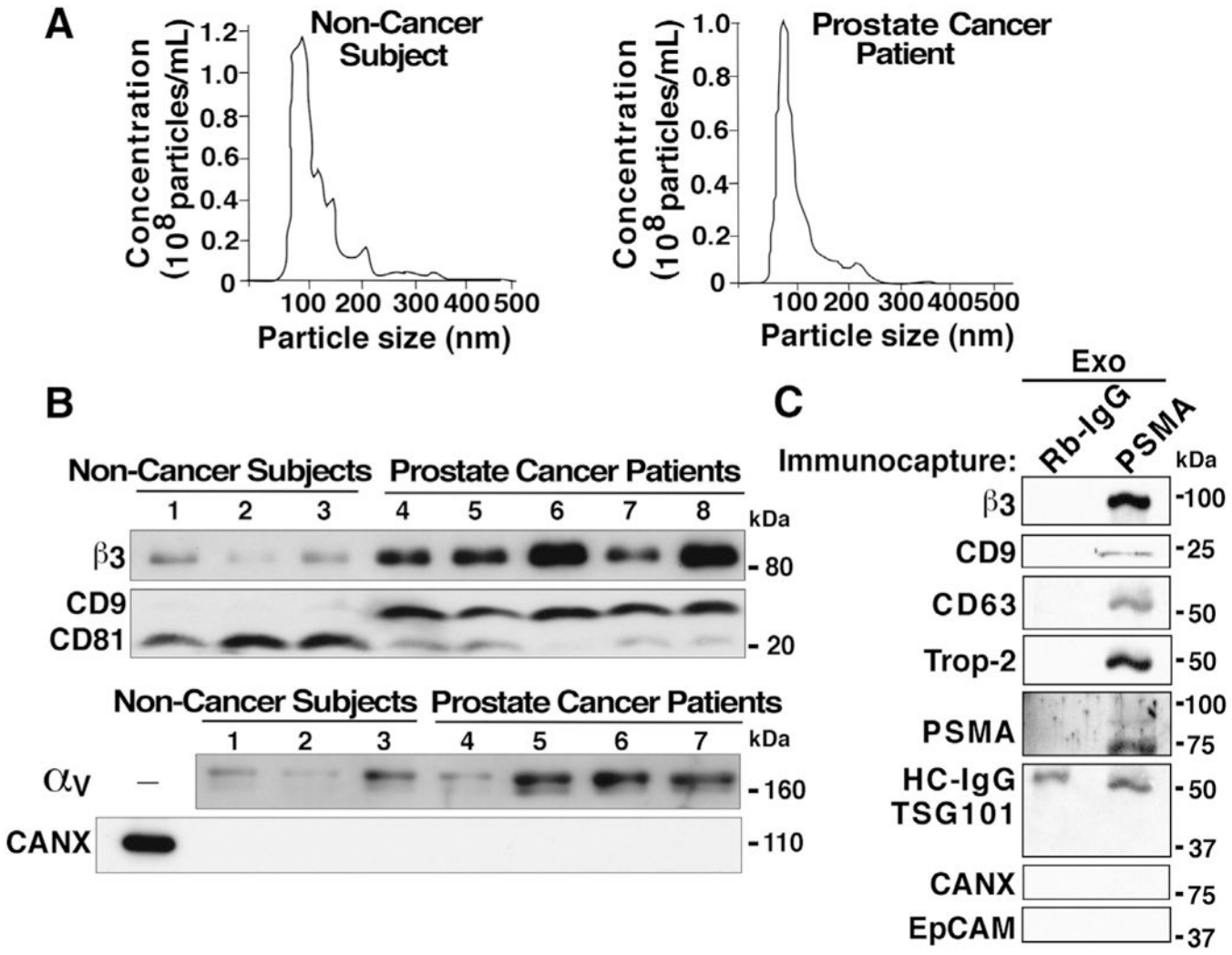

Fig. 4.

Size distribution analysis and differences in β3 integrin levels in ExVs from plasma of prostate cancer patients compared to subjects not affected by cancer. (A) NTA of ExVs isolated by differential ultracentrifugation from plasma of individuals not affected by cancer (left panel) and prostate cancer patients (right panel). (B) IB analysis of β3, CD9, CD81, and αv levels in ExVs isolated by differential ultracentrifugation from plasma of prostate cancer patients compared to age-matched individuals not affected by cancer. CANX was analyzed as a marker absent in exosomes. Lanes 1, 2, and 3: EV lysates isolated after the plasma was pooled from at least two subjects not affected by cancer (total of 7 biological samples represented in 3 lanes); lanes 4–8: EV lysates from individual patients. 30 μg of exosome lysates were loaded in each lane. (C) Iodixanol gradient purified Exosomes (Exo) from prostate cancer patient plasma (pooled from $n = 3$) were immunocaptured with an antibody to Prostate Specific Membrane Antigen (PSMA) or isotype rabbit immunoglobulin (Rb-IgG) conjugated with Dynabeads M-270 epoxy magnetic beads, according to the manufacturer's protocol. The immunocaptured whole exosomes were lysed with RIPA buffer, and lysates were separated by SDS-PAGE (7.5% gel). IB analysis shows expression of β3, CD9 and

CD63 (exosomal markers), Trop-2, and PSMA; in contrast, TSG101 (exosomal marker), CANX and EpCAM were not detected. HC-IgG, heavy chain IgG.

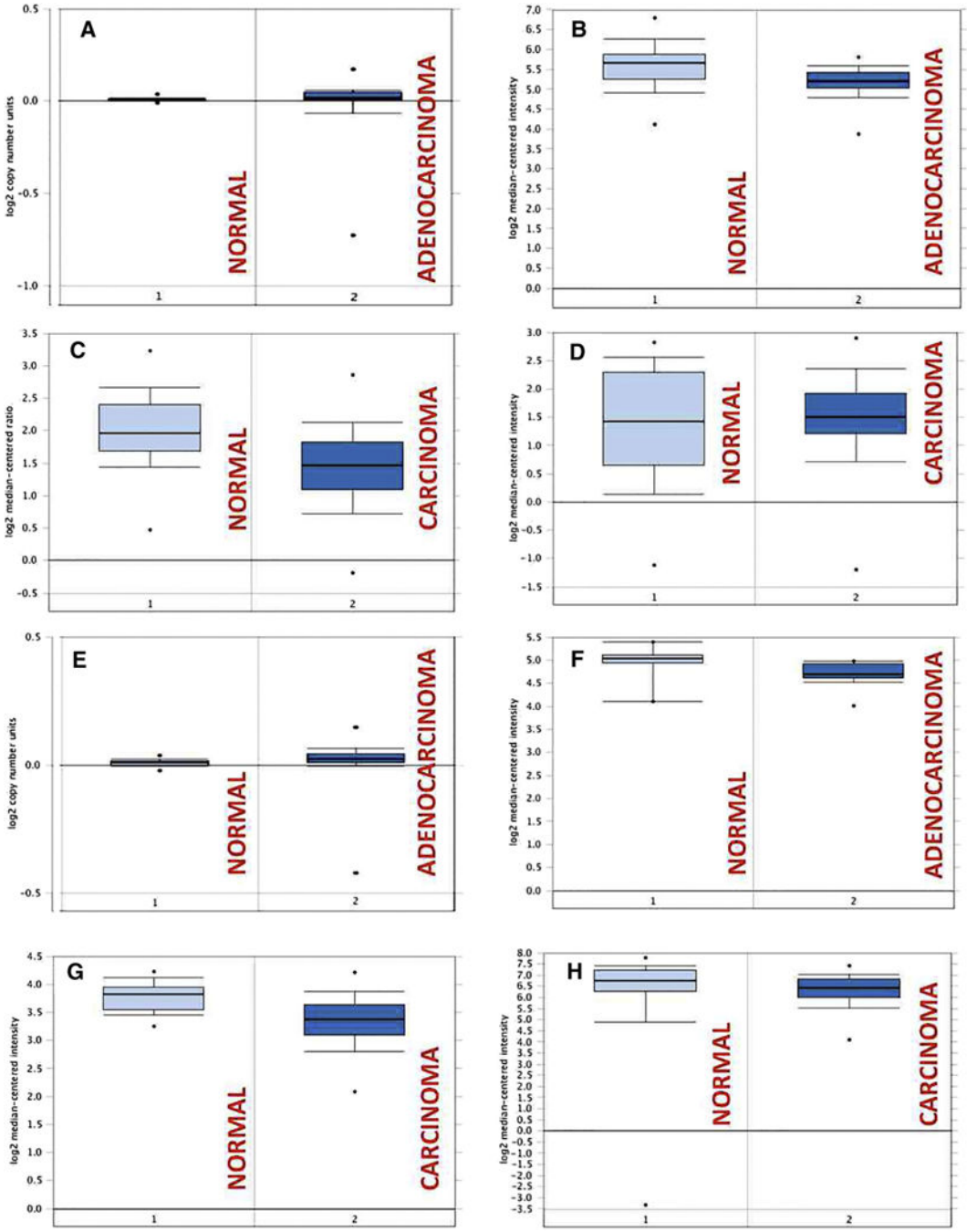

Fig. 5.

Gene expression analysis of CD9 and CD81 in prostate cancer compared to normal samples in publicly available gene expression profiling datasets. (A–D): Gene expression boxplots for CD9. (A) TCGA dataset-prostate adenocarcinoma versus normal. (B) Wallace dataset-prostate adenocarcinoma vs. normal. (C) Lapointe dataset- prostate carcinoma vs. normal. (D) Yu dataset-prostate carcinoma vs. normal. (*E*-H): Gene expression boxplots for CD81. (E) TCGA dataset-prostate adenocarcinoma vs. normal. (F) Vanaja dataset-prostate

adenocarcinoma vs. normal. (G) Taylor dataset-prostate carcinoma vs. normal. (H) Singh dataset- prostate carcinoma vs. normal. 1, Normal; 2, Carcinoma or Adenocarcinoma.

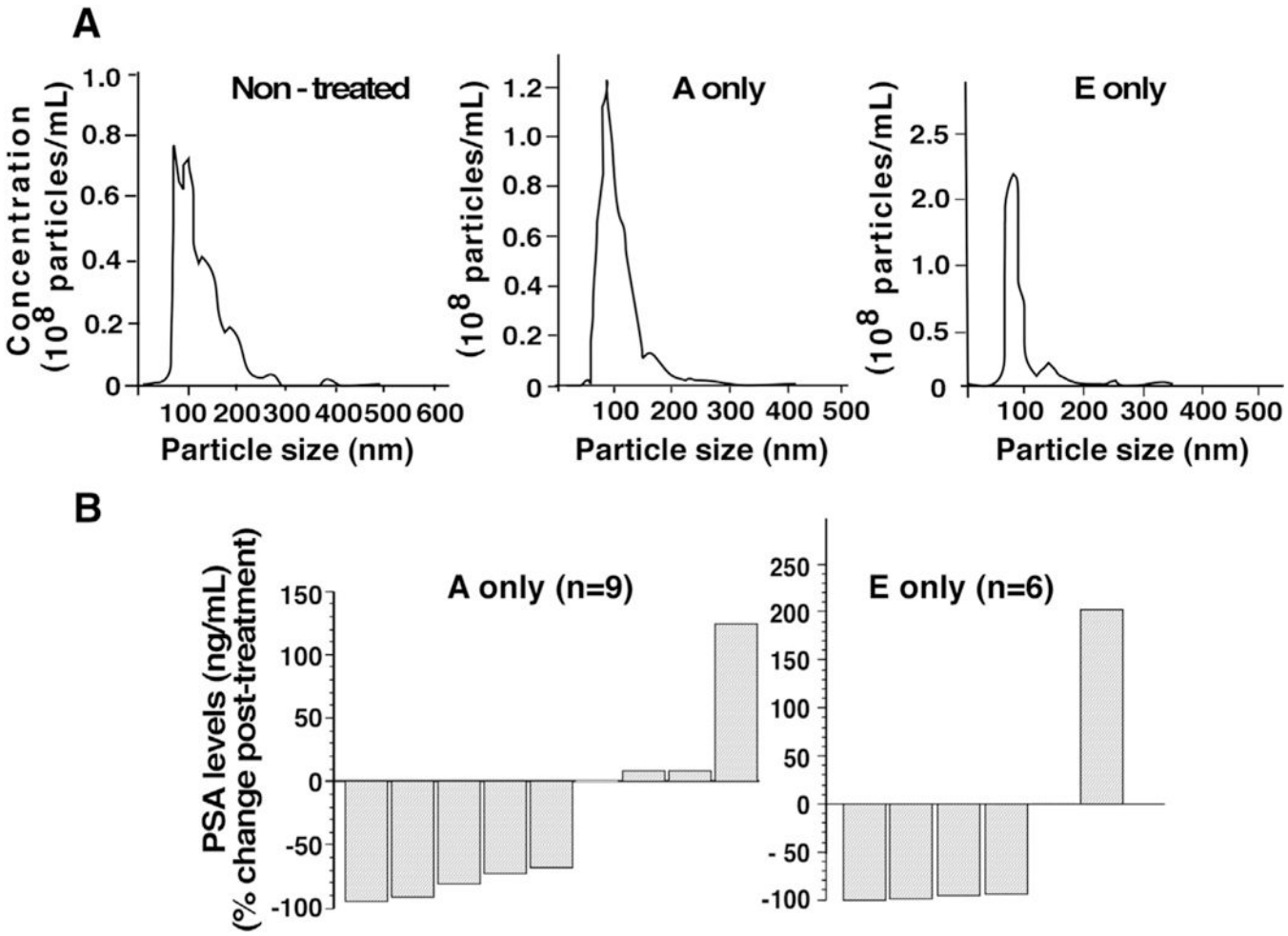

Fig. 6.

Nanoparticle tracking analysis (NTA) of ExVs and PSA levels in serum from prostate cancer patients. (A) The size distribution analysis and concentrations were determined for patients in the following groups: patients that were not treated with abiraterone acetate or enzalutamide (Non-treated), treated with abiraterone acetate only (A only), and treated with enzalutamide only (E only). (B) PSA levels in serum of prostate cancer patients, before and after androgen deprivation therapy (abiraterone acetate or enzalutamide).

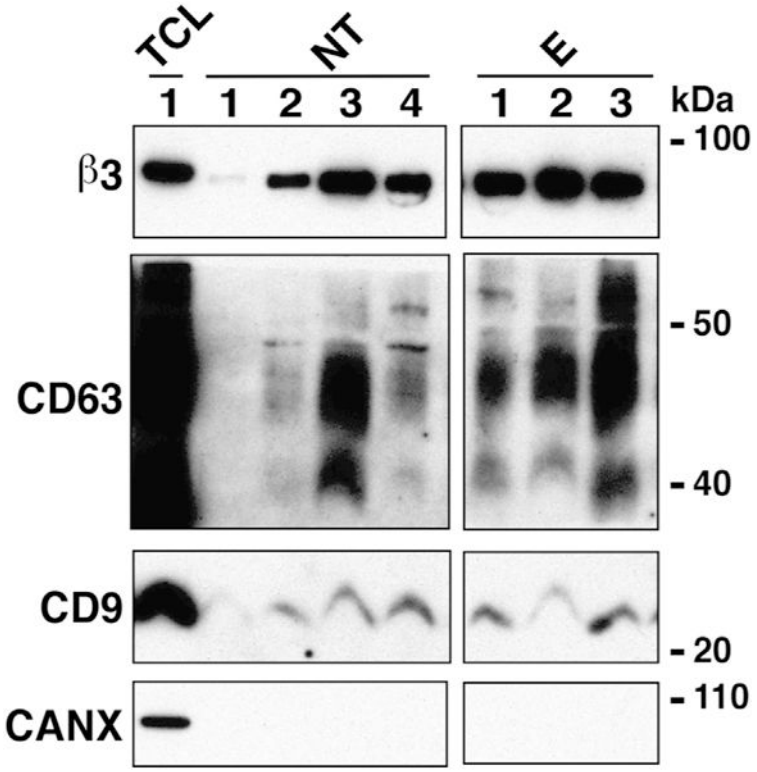

Fig. 7.

β3 integrin levels in plasma of patients treated with enzalutamide (E) compared to patients non-treated (NT) with this drug. IB analysis reveals expression levels of β3 integrin in ExVs derived by differential ultracentrifugation of plasma from patients either non-treated (NT) or treated with enzalutamide (E). CD9, CD63 serve as markers enriched in exosomes and CANX as a marker absent in exosomes. TCL from PC3 cells was used as a positive control for the expression of β3, CD63, CD9, and CANX.